Journal of Macromolecular Science, Part A
Publication details, including instructions for authors and subscription information:
http://www.informaworld.com/smpp/title~content=t713597274

Characterization of Segmental Orientation in Stretched Rubbery Networks by the Stationary Fluorescence Polarization Technique

Jean-Pierre Queslel[a]; Lucien Monnerie[b]; Burak Erman[c]
[a] Manufacture Francaise des Pneumatiques Michelin Centre d'Essais et de Recherche de Ladoux, Clermont-Ferrand Cedex, France [b] Laboratoire de Physicochimie Structurale et Macromoléculaire E.S.P.C.I., Paris Cedex 05, France [c] Polymer Research Center Bogazici, University, Istanbul, Turkey

To cite this Article Queslel, Jean-Pierre , Monnerie, Lucien and Erman, Burak(1989) 'Characterization of Segmental Orientation in Stretched Rubbery Networks by the Stationary Fluorescence Polarization Technique', Journal of Macromolecular Science, Part A, 26: 1, 93 — 123
To link to this Article: DOI: 10.1080/00222338908053845
URL: http://dx.doi.org/10.1080/00222338908053845

J. MACROMOL. SCI.–CHEM., A26(1), pp. 93-123 (1989)

CHARACTERIZATION OF SEGMENTAL ORIENTATION IN STRETCHED RUBBERY NETWORKS BY THE STATIONARY FLUORESCENCE POLARIZATION TECHNIQUE

JEAN-PIERRE QUESLEL

Manufacture Francaise des Pneumatiques Michelin
Centre d'Essais et de Recherche de Ladoux
63040 Clermont-Ferrand Cedex, France

LUCIEN MONNERIE

Laboratoire de Physicochimie Structurale et Macromoléculaire
E.S.P.C.I.
10 rue Vauquelin, 75231 Paris Cedex 05, France

BURAK ERMAN

Polymer Research Center
Bogazici University, Bebek, 80815
Istanbul, Turkey

ABSTRACT

In 1978, Jarry and Monnerie showed that the stationary fluorescence polarization technique can be used to measure orientation in mobile uniaxially symmetric systems. Determination of segmental orientation in stretched rubbery networks may then serve to validate and improve elaborated models of rubberlike elasticity in conjunction with stress-strain measurements. As a preliminary, the basic principles of the fluorescence polarization technique and its application to investigation of molecular behavior of mobile anisotropic networks are described. Then, the theory of segmental orientation of real networks with constraints on junctions, proposed by Erman and Monnerie in 1985, is reviewed. Illustrative data on elasticity and orientation behavior of

cis-1,4-polyisoprene networks are consistent with theoretical predictions. The effect of temperature on segmental orientation is attributed to changes in the configurational factor expressed in the theory. In fluorescence polarization experiments, only the orientation behavior of the labeled species is observed. Thus, comparison of the behavior of anthracene end-labeled and center-labeled chains has revealed that dangling chains are very strongly orientationally coupled to network chains. It is, however, a local effect which does not imply an overall anisotropy of dangling chains at equilibrium. Orientational coupling between flexible probes of different lengths and polymer matrix was also investigated and compared with that of rigid probes.

I. INTRODUCTION

Relationships between structure and properties of bulk polymers are generally established by analysis of macroscopic mechanical behavior with theoretical models.

In the field of rubberlike elasticity, new models were recently proposed which can indeed be used to characterize the structure of real elastomeric networks in view of their mechanical properties [1, 2]. However, several parameters are necessary to describe the relationship between molecular and macroscopic deformations and, therefore, stress-strain measurements are generally not sufficient to judge without ambiguity the validity of these elaborate theories. Another possible test consists in measuring molecular orientation in stretched rubbery networks. With this in view, the photoelastic properties of rubbers have been widely investigated [3-5]. However, birefringence data suffer from the fact that segmental polarizability is affected by its immediate environment.

Recent developments in spectroscopic techniques permit accurate measurement of orientation of structural units in deformed polymeric systems [6, 7]. For this purpose, spectroscopic techniques, such as small-angle neutron scattering, infrared dichroism, ^{2}H-NMR spectroscopy, and fluorescence polarization are particularly suitable [6]. Small-angle neutron scattering yields information either on the molecular dimensions of the whole chain or on the structure of part of the chain, whereas infrared dichroism, ^{2}H-NMR spectroscopy, and fluorescence polarization applied to stretched samples lead to information about chain-segment orientation. It is worth noting that the transition moments of the labels involved in fluorescence polarization are not sensitive to their immediate environment. In this paper we deal exclusively with fluorescence polarization.

After presenting the stationary fluorescence polarization technique, we will consider its application to the study of segmental orientation in elastomeric networks stretched far above their glass transition temperature. Corresponding models that have been proposed recently are reviewed and then serve to analyze experimental results.

II. ORIENTATION DISTRIBUTION FUNCTION

The degree of molecular segmental orientation in a deformed amorphous polymeric network is obtained from the orientational distribution function. This distribution is represented by a function $f(\theta_x)$, where θ_x is the angle between unit vectors affixed to chain segments and the laboratory fixed axis denoting the direction of stretch. The function $f(\theta_x)$ can be expanded in terms of Legendre polynomials in $\cos \theta_x$ as follows:

$$f(\theta_x) = \sum_l b_l P_l (\cos \theta_x) \tag{1}$$

with

$$b_l = \left[\left(\frac{1}{2}\pi\right)(2l+1)/2\right] \langle P_l (\cos \theta_x)\rangle, \tag{2}$$

where $\langle P_l (\cos \theta_x)\rangle$ is the value of $P_l (\cos \theta_x)$ averaged over the distribution. The average of the second Legendre polynomial is defined as

$$S_x \equiv \langle P_2 (\cos \theta_x)\rangle = \frac{1}{2}\langle 3 \cos^2 \theta_x - 1\rangle, \tag{3}$$

$$\langle \cos^2 \theta_x \rangle = \int_0^\pi f(\theta_x) \cos^2 \theta_x \sin \theta_x \, d\theta_x. \tag{4}$$

It has been shown that, in most cases, the determination of P_2 is sufficient for a uniaxial distribution.

III. THE FLUORESCENCE POLARIZATION (FP) TECHNIQUE

A. Principles

Fluorescent molecules have the property of reemitting part of the energy acquired by absorption of luminous radiation in the form of visible light. After illuminating with a very short pulse at time t_0, the fluorescent light

emitted at time $t_0 + u$ is proportional to $\exp(-u/\tau)$, where τ is the mean lifetime of the excited state (usually called the fluorescent lifetime). The most frequent values range from 10^{-9} to 10^{-7} s. When absorbing light of a suitable wavelength, a molecule behaves as an electric dipole oscillator with a fixed orientation with respect to the geometry of the molecule. Such an equivalent oscillator is termed an absorption transition moment, M_0. In the same way, for fluorescence emission we have an emission transition moment, M. When such a molecule receives an incident beam polarized along the P direction, the absorption probability is proportional to $\cos^2 \gamma$, where γ is the angle between P and M_0. In the same way, the fluorescence intensity measured through an analyzer, A, is proportional to $\cos^2 \delta$, where δ is the angle between M and A. Thus, for the P and A directions of the polarizer and the analyzer, the observed luminescence intensity is proportional to $\cos^2 \gamma \cos^2 \delta$. Owing to the lack of phase correlation between excitation and emission light, fluorescence emission can be described as resulting from three independent radiations, respectively polarized along the X, Y, and Z laboratory axes with intensities I_X, I_Y, and I_Z. The Curie symmetry principle, applied to excitation light polarized along Z, leads to $I_X = I_Y$. The fluorescence polarization is characterized by the emission anisotropy:

$$r = (I_{\parallel} - I_{\perp})/(I_{\parallel} + 2I_{\perp}), \tag{5}$$

where $I_{\parallel}$ and $I_{\perp}$ correspond to the fluorescence intensity obtained with an analyzer direction parallel or perpendicular, respectively, to that of the polarizer.

When dealing with an isotropic set of fluorescence molecules for which the relaxation times of the molecular motions are in the range of the fluorescence lifetime, FP yields information on the mobility of the molecules. This high-frequency mobility appears in polymers at temperatures above T_g(DSC) + 50°C [8].

B. Orientation of Uniaxially Symmetric Systems

For our present purpose we are mainly interested in the use of FP to look at the orientation distribution of fluorescence molecules. The transition moments in both absorption and emission are assumed to coincide with a molecular axis M of the molecule, the direction of which is specified by the spherical polar angle $\Omega = (\theta, \beta)$ in the reference frame (Fig. 1). In the treatment [9] the following are then introduced: the angular functions $N(\Omega_0, t_0)$; the orientation distribution of M at time t_0 (M_0 in Fig. 1); and $P(\Omega, t; \Omega_0, t_0)$,

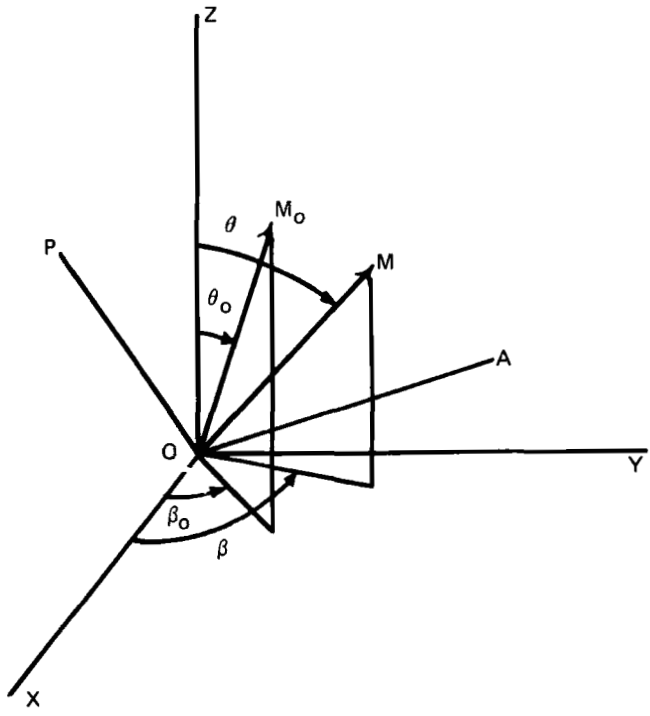

FIG. 1. Illustration of the angles which define the orientation of the molecular axis M_0 at time t_0 and M at time $t_0 + u$ with respect to the fixed frame OXYZ.

the conditional probability density of finding a vector M at position Ω at time t which was at position Ω_0 at time t_0. After illuminating the samples by a linearly polarized short pulse of light at t_0, the intensity emitted at time $(t_0 + u)$ for the P and A directions of polarizer and analyzer is given by

$$i(P,A,t_0,u) = K\int\int N(\Omega_0,t_0)P(\Omega,t_0+u;\Omega_0,t_0)\cos^2(P,M_0)\cos^2(A,M)$$
$$\exp(-u/\tau)d\Omega_0 d\Omega, \qquad (6)$$

where K is an instrumental constant. In this expression, t_0 corresponds to the macroscopic evolution of the sample, whereas u corresponds to a microscopic reorientational motion in the scale of the fluorescence lifetime τ. In most cases the t_0 dependence of N and P can be ignored within the time τ ($\sim 10^{-8}$ s),

and the fluorescence intensity emitted under continuous excitation is given by

$$i(P,A,t_0,\tau) = \int_0^\infty i(P,A,t_0 + u)du \tag{7}$$

In the case of a uniaxially symmetric distribution of the molecular axes M, the intensities corresponding to the P and A directions lying along the fixed-frame axes (Z corresponds to the symmetry axis) can be conveniently expressed through the following quantities:

$$G_{20}^{(0)} = \frac{1}{2}\langle 3\cos^2\theta_0 - 1\rangle,$$

$$G_{02}^{(0)} = \frac{1}{2}\langle 3\cos^2\theta - 1\rangle,$$

$$G_{22}^{(0)} = \frac{1}{4}\langle 3\cos^2\theta_0 - 1)(3\cos^2\theta - 1)\rangle,$$

$$G_{22}^{(1)} = \frac{9}{16}\langle \sin\theta_0\cos\theta_0\sin\theta\cos\theta\cos(\beta - \beta_0)\rangle,$$

$$G_{22}^{(2)} = \frac{9}{64}\langle \sin^2\theta_0\sin^2\theta\cos 2(\beta - \beta_0)\rangle. \tag{8}$$

Thus, for example:

$$i(X,X) = \frac{K}{9}(1 - G_{20}^{(0)} - G_{02}^{(0)} - G_{22}^{(0)} + 8G_{22}^{(2)}),$$

$$i(Z,Z) = \frac{K}{9}(1 + 2G_{20}^{(0)} + 2G_{02}^{(0)} + 4G_{22}^{(0)}),$$

$$i(Z,X) = \frac{K}{9}(1 + 2G_{20}^{(0)} - G_{02}^{(0)} - 2G_{22}^{(0)}). \tag{9}$$

In uniaxial mobile systems, i.e., polymers at a temperature above T_g(DSC) + 50°C, both orientation and mobility contribute to the fluorescence polarization, and the two effects have to be separated from the measured intensities. This is possible if we assume that, during the fluorescence lifetime ($\sim 10^{-8}$ s), the orientation distribution does not change [9]. Nevertheless, special equipment is required, and only $P_2(\cos\theta)$ can be obtained by the measurement of fixed intensities, $i(P,A)$, corresponding to P and A directions which are not contained in the same plane. On the other hand, the mean amplitude of the

motion performed during the fluorescence lifetime, $M(\tau)$, is available from the data [10]:

$$\bar{M}(\tau) = \int_0^\infty M(u)e^{-u/\tau}du/\tau, \tag{10}$$

with

$$M(u) = <(3\cos\theta(u) - 1)/2>, \tag{11}$$

where $\theta(u)$ is the angle through which the M-axis rotates between t_0 and $t_0 + u$.

An apparatus to measure simultaneously the convenient set of intensities $i(P,A)$ has been developed [11] and is represented in Fig. 2. Values of the second moment S_x are obtained after correcting for the effect of the delocalization of the transition moments and for birefringence of the sample [9]. This fluorescence polarization apparatus permits simultaneous measurements of stress and orientation during uniaxial stretching at constant crosshead speed, $V = 50$ mm/min, and various temperatures.

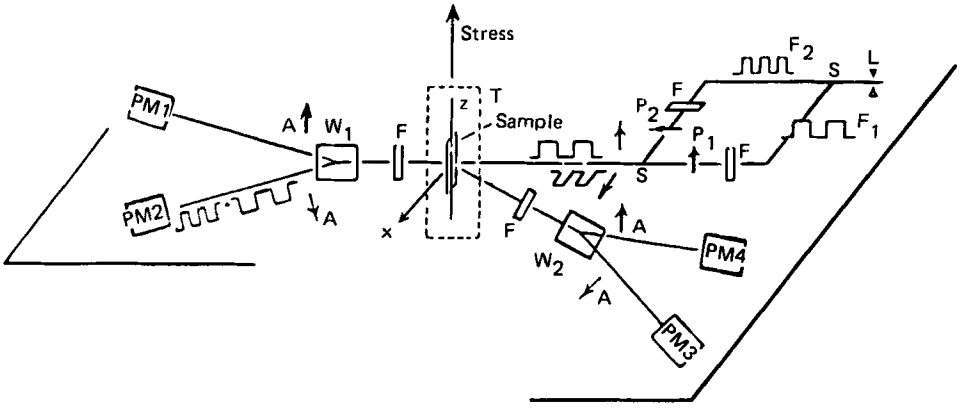

FIG. 2. Optical equipment: L, mercury lamp; S, beam splitter; f_1, f_2, modulation frequencies of the mechanical choppers; F, optical filter; P_1, P_2, polarizers; W_1, W_2, Wollaston prisms; A, analyzing directions; PM, photomultiplier; T, temperature chamber.

C. Fluorescent Labels and Probes

The use of luminescent polarization for studying orientation of polymer chains requires extrinsic luminescent molecules. Indeed, many polymers do not exhibit any luminescence owing to their chemical structure. Even when the polymer chain contains luminescent groups, as polystyrene or poly(vinylnaphtalene), the energy transfer processes occurring between these groups lead to an almost complete depolarization of the emitted light, negating any possibility of studying the chain orientation.

Nevertheless, the orientation of stretched rubbers can be studied through extrinsic probes incorporated in the polymer matrix or through luminescent groups covalently bound to the polymer chain referred to as "labels."

In choosing a luminescent probe or label, several features have to be considered. First, it is important that the electronic transition between the ground state and the first excited state could be excited without exciting any other transition. This is required for an unambiguous definition of the transition moments involved. In particular, molecules where the π-π^* and n-π^* absorption bands overlap must be avoided, for these transitions correspond to absorption transition moments which are, in aromatic molecules for example, in-plane and out-of-plane polarized, respectively. Second, the fundamental anisotropy, r_0, must be high in order to yield easily measurable polarization. In the same way, it is convenient to get a high quantum yield of luminescence which does not vary greatly over a wide range of changes in the properties of the medium (temperature, solvent nature, chemical structure of polymers). Finally, the absorption and emission bands must occur in a spectral range suitable for experimentation, typically above 350 nm.

In order to avoid any energy transfer between fluorescent molecules, their concentration must be sufficiently low, approximately 10 μmol/L for the samples presented in this paper. In this concentration range the luminescence intensity increases linearly.

1. Labels

Various types of labeling can be performed: along the main chain, at the chain end, or on a side chain, depending on the chemical reaction used and on the chemical structure of the polymer chain. For any labeling, one important feature is the position of the transition moments relative to the chain backbone. Indeed, it is necessary to covalently bind the luminescent group in such a way that rotations of its transition moments independent of the chain backbone are avoided.

In the case of fluorescence, the most appropriate label is the anthracene

group, for its optical properties are very convenient and many reactive derivatives are available for labeling [12].

This paper addresses the orientation behavior of active chains and dangling chain ends in stretched *cis*-1,4-polyisoprene networks.

Anionic polyisoprene chains were labeled in their center by using a method analogous to that reported previously for polystyrene [13]. Monofunctional "living" chains of molecular weight 300 000 were synthesized and deactivated by 9,10-bis(bromomethyl)anthracene. Each of the resulting chains of double molecular weight contains a dimethyleneanthracene (DMA) fluorescent group at its center. Thus the fluorescent transition moment, the orientation of which is measured, lies along the chain axis, as shown in Fig. 3(a).

Polyisoprene chains were labeled at their ends by deactivation of monofunctional "living" chains of molecular weight 600 000 with monobromomethylanthracene.

The center-labeled or the end-labeled polymer (1%) and the matrix (99%), carefully purified by extraction with ethanol, were mixed in solution.

2. Probes

Various probes can be used for fluorescence polarization studies. The advantage of using probes instead of labels is that they can be inserted into the polymer materials without chemical process. The specific aim of one study reviewed in this paper was to analyze orientational correlations between unattached flexible probes of different lengths, rigid probes, and network chains at various degrees of uniaxial extension of the network.

The flexible linear 9,10-di-*n*-alkylanthracene probes used in the study were synthesized in our laboratory following an original method [14]. They are shown in Fig. 3(b). In the following, we abbreviate these compounds as C_n.

Three rigid probes of varying size were also employed. Their formula and transition moments are shown in Fig. 3(c).

Crosslinked polymer samples were swollen with solutions of the probes in benzene and then dried *in vacuo*.

IV. THEORY OF SEGMENTAL ORIENTATION IN AMORPHOUS POLYMER NETWORKS

As mentioned in the Introduction, the study of segmental orientation can be used to validate models of rubberlike elasticity derived from experimental mechanical behavior of rubber networks. The elaboration of these models requires a topological description of the network structure and the establish-

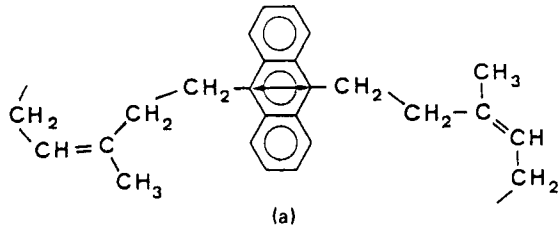

(a)

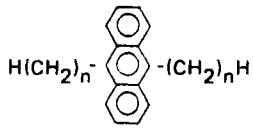

(b)

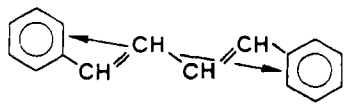

Diphenylbutadiene (DPBD)

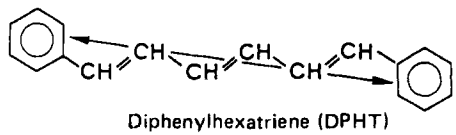

Diphenylhexatriene (DPHT)

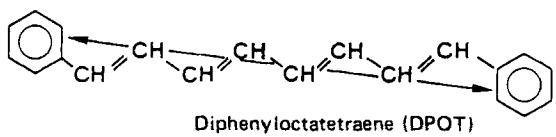

Diphenyloctatetraene (DPOT)

(c)

FIG. 3(a). 9,10-Dimethyleneanthracene-labeled polyisoprene. Fig. 3(b). 9,10-Di-*n*-alkylanthracene probes C_n with $n = 2, 3, 4, 6, 10, 12, 14, 16$. Fig. 3(c). Rigid probes.

ment of a stress-strain relationship for this structure. We will review these two aspects of rubberlike elasticity and then a theory of segmental orientation proposed recently by Erman and Monnerie [15].

A. Network Structure

Although model networks, i.e., networks of controllable and independently known structure, are well suited to test rubberlike elasticity models [16, 17], most studies and actual applications involve statistically crosslinked networks (for example, those which have been radiation or peroxide cured). In these latter cases, topological description is very difficult, but may be treated with a probabilistic formalism [18-20].

A universal quantity, called the cycle rank ξ and encompassing all imperfections like loops and dangling ends, was proposed by Flory [21]. It is defined as the number of independent circuits which have to be cut to reduce the mesh (network) structure to an acyclic tree. The number of effective junctions μ is directly related to the network cycle rank ξ and functionality φ by the following equation [22]:

$$\xi = (\varphi/2 - 1)\mu. \tag{12}$$

To form a network, it is first necessary to connect linear chains into a tree. The quantity μ is the difference between the total number of junctions in the final network and the number of junctions in this acyclic structure. ξ and μ are the two topological quantities that are used in the elasticity model presented hereafter.

B. Stress-Strain Relationship

The high deformability of an elastomer and the elastic force generated by deformation stem from the essentially unlimited number of configurations accessible to long molecular chains. This versatility has been characterized in numerous theoretical investigations on typical polymer chains. They have shown that the Gaussian approximation for the end-to-end distance distribution function should be quite satisfactory for chains consisting of 100 or more bonds [21, 23, 24]. The non-Gaussian effect generally exists only in the very high, limited extensibility region of deformation.

Stress-strain properties of elastomeric networks in the Gaussian region can be explained only through an understanding of the relationship between molecular chain deformation and macroscopic strain. Two basic models of

Gaussian networks have been proposed for this purpose [22, 25]. In the affine network, displacements of junctions and chain vectors are a simple linear function of the macroscopic strain [26]. In the phantom network, on the other hand, chains are devoid of material properties [27], and macroscopic constraints operate only on the periphery of the network. Other junctions fluctuate without restraints from neighboring chains. In both cases, the reduced stress measured in uniaxial extension is predicted to be independent of deformation. This reduced stress is conventionally defined as [28]

$$[\tau] \equiv \nu_2^{-1/3}(\tau_x - \tau_y)/(\alpha^2 - \alpha^{-1}), \tag{13}$$

where $\tau_x - \tau_y$ is the difference between the principal components of the equilibrium true stress along the longitudinal (x) and the lateral (y) directions of deformation, α is the ratio of the swollen deformed length to the swollen undeformed length, and ν_2 is the volume fraction of polymer in the swollen network. Departures from this behavior were reported very early in the study of rubberlike elasticity [29, 30]. These observations have shown that the reduced stress decreases markedly with elongation and with dilation by swelling, and have suggested that the limiting value of the reduced stress at high elongation or high dilation is a fundamental characteristic of a given network. It became apparent later [31] that this quantity was the phantom network modulus $\xi kT/V$, where ξ/V is the cycle rank density of the swollen network [21, 22], k is the Boltzmann constant, and T is the absolute temperature.

These observations then gave rise to phenomenological equations like the Mooney-Rivlin expression, i.e.,

$$[\tau] = 2C_1 + 2C_2/\alpha. \tag{14}$$

In real networks, diffusion of junctions about their mean positions may be severely restricted by neighboring chains sharing the same region of space. Real networks present strong chain overlapping. Intermolecular steric hindrance on chain motion, commonly termed "entanglements," has long been recognized to be the origin of departures from phantom and affine predictions. Different formalisms were proposed to include these intermolecular effects in the rubberlike elasticity analysis at thermodynamic equilibrium [25]. In the one due to Flory and Erman [2], entanglements are embodied as domains of constraints acting as restrictions of junction fluctuations. These domains can be initially represented as spheres. They are transformed to ellipsoids by the deformation. In uniaxial extension, the main axes of these ellipsoids are along the direction of stretching. Thus fluctuations in-

crease in the direction along which the stress is measured. The behavior of real networks then tends to that of phantom networks with large fluctuations in the limit of infinite deformation. The C_2 effect, observed experimentally in uniaxial tensile tests of amorphous rubbers, results from the transformation of fluctuations with strain in the manner stated above and is predicted by this molecular model of constraints. The principal parameter κ of the theory is defined as the ratio of the mean-square radius of the fluctuations of the junctions in the phantom network $<(\Delta R)_{ph}{}^2>$ to the mean-square radius $<(\Delta s)^2>_0$ of the Gaussian domains of constraints in the undistorted network, i.e.,

$$\kappa = <(\Delta R)_{ph}{}^2>/<(\Delta s)^2>_0. \tag{15}$$

The parameter κ has been postulated to depend on the degree of interpenetration in the network, which is well supported by experiments [32, 33]. A second parameter ζ is believed to reflect the effect of inhomogeneities in the network topology which perturb the affine transformation of constraint domains with macroscopic deformation [34].

The molecular theory of elasticity outlined above predicts the following expression for the difference between the principal components of the true stress along the longitudinal (x) and the lateral (y) directions of deformation [2]:

$$\tau_x - \tau_y = (\xi kT/V)\left\{\lambda_x{}^2 - \lambda_y{}^2 + (\mu/\xi)[\lambda_x{}^2 K(\lambda_x{}^2) - \lambda_y{}^2 K(\lambda_y{}^2)]\right\}, \tag{16}$$

where

$$K(\lambda_t{}^2) = B_t[\dot{B}_t(B_t+1)^{-1} + g_t(\dot{g}_t B_t + g_t\dot{B}_t)(g_t B_t + 1)^{-1}], \tag{17}$$
$$t = x, y$$

with

$$B_t = (\lambda_t - 1)(\lambda_t + 1 - \zeta\lambda_t{}^2)/(1+g_t)^2,$$
$$g_t = \lambda_t{}^2[\kappa^{-1} + \zeta(\lambda_t - 1)],$$
$$\dot{B}_t \equiv \partial B_t/\partial\lambda_t{}^2 = B_t\left\{[2\lambda_t(\lambda_t - 1)]^{-1} + (1 - 2\zeta\lambda_t)[2\lambda_t(1 + \lambda_t - \zeta\lambda_t{}^2)]^{-1} - 2\dot{g}_t(1+g_t)^{-1}\right\},$$
$$\dot{g}_t \equiv \partial g_t/\partial\lambda_t{}^2 = \kappa^{-1} - \zeta(1 - 3\lambda_t/2). \tag{18}$$

In Eq. (16), ξ/V represents the cycle rank (number of independent circuits in the network) density of the swollen network [21, 22], k is the Boltzmann constant, T is the absolute temperature, and μ is the number of effective junctions.

The deformation ratios λ_x and λ_y characterizing the deformation of the swollen network relative to the unswollen, undeformed state are related to α by the following equations:

$$\lambda_x = \nu_2^{-1/3}\alpha,$$
$$\lambda_y = \nu_2^{-1/3}\alpha^{-1/2}. \tag{19}$$

The phantom network limit is reached when $\kappa \to 0$ and $\kappa\zeta \to 0$ [2]. Equation (16) then simplifies to

$$(\tau_x - \tau_y)_{ph} = (\xi kT/V)(\lambda_x^2 - \lambda_y^2). \tag{20}$$

The affine limit corresponds to $\kappa \to \infty$ and $\zeta \to 0$.

This Flory and Erman model was indeed successful in accounting for the relationships of stress to strain for a variety of strains for typical elastomers throughout ranges accessible to experiments [33-36].

C. Segmental Orientation

Previous treatments of segmental orientation were based on the affine or phantom model [37, 38]. The molecular theory of real networks presented above has been recently applied to the analysis of segmental orientation by Erman and Monnerie [15]. The expression for the second moment S_x of the orientation function for Gaussian networks is conveniently separated into two factors: a configurational factor D, which represents the statistical properties of chains, and a strain function $F(\alpha)$, which relates the orientation to macroscopic deformation:

$$S_x = DF(\alpha). \tag{21}$$

For a long, freely-jointed chain formed with N statistical segments:

$$D = \frac{1}{5}N. \tag{22}$$

However, in real networks, chains are not freely jointed. Furthermore, chain segments are locally subject to orientational correlations from segments of the neighboring chains in the bulk state. These local intermolecular orientational correlations affecting local orientation of segments but not the overall chain configurations have been observed in birefringence [33, 39] and fluorescence polarization [40, 41] experiments and have been attributed to hindrance of rotations of neighboring segments about each other due to intermolecular steric constraints (uncrossability of chains) and to alignment of neighboring chain segments with respect to each other due to anisotropic intermolecular dispersive forces [42]. In the case of weak local correlations, it can be shown [15] that the configurational factor for the chain in real network, D, is the sum of the configurational factor for the free chain, D_0, and an intermolecular contribution, D_{int}:

$$D = D_0 + D_{\text{int}} \tag{23}$$

The configurational factor D_0 for a free chain is given by Nagai's treatment [43]:

$$D_0 = (3\langle r^2 \cos^2 \Phi\rangle_0/\langle r^2\rangle_0 - 1)/10, \tag{24}$$

where Φ is the angle between a labeled segment and the chain end-to-end vector r. Angular brackets with the subscript zero denote the ensemble average for a free chain in the unperturbed state. The expression given by Eq. (24) reduces to that given by Eq. (22) for a freely jointed chain.

The value of D_0 for a given chain may be conveniently evaluated by the rotational isomeric state formulation. Rational calculation of D_{int} in terms of molecular parameter awaits further work.

The strain function depends on the transformations of chain dimensions with deformation in real networks. According to the model proposed by Flory and Erman [2], the elements of the molecular deformation tensor Λ^2 can be expressed as the sum of contributions from the phantom network, $\Lambda_{\text{ph}}{}^2$ and from the constraints, $\Lambda_c{}^2$:

$$\Lambda_t{}^2 = \Lambda_{t,\text{ph}}^2 + \Lambda_{t,c}^2, \qquad t = x, y, z. \tag{25}$$

In addition to the deformation of the chains associated with the alteration of their chain vectors under strain, it is necessary to consider the action of the junctions on the constraint domains surrounding them. The junction and its domain are coupled elastic elements. Nonaffine transformation of the fluctua-

tion domains of junctions in the presence of chain connectivity creates an additional strain field in the medium around each junction. A domain deformation tensor Θ^2 can be introduced in analogy with Λ^2. Θ^2 relates the mean deformation (according to ensemble distribution) of the junction constraint domains in the deformed, connected network to that in the absence of connectivity. Consequently, the state of microscopic deformation in a real network is the sum of the molecular deformation tensor, Λ^2, and the junction domain deformation tensor, Θ^2.

The first contribution to the strain function is expressed by the molecular deformation tensor Λ^2:

$$F_1(\lambda) = \Lambda_x^2 - (\Lambda_y^2 + \Lambda_z^2)/2. \tag{26}$$

The second contribution arises from the distortion of the junction constraint domains. Depending on the extent of distortion, a chain surrounding a given junction has to reorganize at a scale corresponding to the size of its constraint domain. This results in an additional orientation of the segment present in the domain proportional to the local domain deformation tensor Θ^2. In analogy with Eq. (26), the second contribution to the strain function may be expressed as

$$F_2(\Lambda) = e[\Theta_x^2 - (\Theta_y^2 + \Theta_z^2)/2], \tag{27}$$

where the parameter e denotes the strength of reaction of orienting chain segments to the distortion of junction constraint domain. The resulting strain function is the sum of F_1 and F_2:

$$F(\lambda) = F_1(\lambda) + F_2(\lambda). \tag{28}$$

According to the theory, the components of the microscopic deformation tensors Λ^2 and Θ^2 are related to the macroscopic deformation tensor λ by

$$\begin{aligned} \Lambda_t^2 &= \left(1 - \frac{2}{\varphi}\right)\lambda_t^2 + \frac{2}{\varphi}(1 + B_t) \\ \Theta_t^2 &= 1 + g_t B_t \end{aligned} \tag{29}$$

Using Eqs. (29) in Eqs. (27) and (28), and substituting in Eq. (21) leads to the following expression for S_x:

$$S_x = (1 - 2/\varphi)\nu_2^{-2/3} D\left\{\alpha^2 - \alpha^{-1} + 2\nu_2^{2/3}(\varphi - 2)^{-1}[B_x - B_y + (\varphi e/2)(g_x B_x - g_y B_y)]\right\}. \quad (30)$$

For a phantom network, the term in square brackets in Eq. (30) vanishes. Therefore

$$S_{x,\mathrm{ph}} = (1 - 2/\varphi)\nu_2^{-2/3} D(\alpha^2 - \alpha^{-1}). \quad (31)$$

The difference between S_x and $S_{x,\mathrm{ph}}$ reflects the effect of constraints on segmental orientation in networks.

In analogy with the reduced stress, the reduced orientation function in uniaxial extension may be defined as

$$[S_x] \equiv \nu_2^{2/3} S_x/(1 - 2/\varphi)(\alpha^2 - \alpha^{-1}) = DS_x/S_{x,\mathrm{ph}}. \quad (32)$$

The limit of $[S_x]$ in the infinite range of deformation is the configurational factor

$$\lim_{\alpha^{-1}\to 0} [S_x] = D. \quad (33)$$

V. STUDIES OF SEGMENTAL ORIENTATION IN UNIAXIALLY STRETCHED POLYISOPRENE NETWORKS

With the improved technique of fluorescence polarization described in Section III, the magnitude of the configurational factor and the form of the strain function for amorphous networks may be determined accurately.

We have investigated orientation behavior of different labels and probes in amorphous *cis*-polyisoprene networks [40, 44-46].

The networks which contain active center-labeled chains were used to test the theory of segmental orientation presented in Section IV. Networks with end-labeled chains, flexible, or rigid probes have served to measure the degree of orientational coupling in the polymer.

A. Orientation of Center-Labeled Chains and Comparison with Theory

Unimodal networks (Samples A and B) were formed from an anionic commercial polyisoprene, Shell IR 307, with a high *cis*-1-4 configuration (92% *cis*,

5% *trans*) (T_g(DSC) = -60°C) of high molecular weight ($\bar{M}_n = 46.3 \times 10^4$, $\bar{M}_w = 182 \times 10^4$).

Bimodal networks (Samples C and D) were formed from blends of 75 wt% of IR 307 and 25 wt% of polyisoprene chains of low molecular weight ($\bar{M}_n = 50 \times 10^3$), the microstructure of which is similar to that of IR 307.

The center-labeled chains (see Section III-C-1) and the matrix, carefully purified by extraction with ethanol, were mixed in solution. Samples were molded and crosslinked with dicumyl peroxide. Curing time and temperature were adjusted to obtain different crosslinking densities which were characterized by the average molecular weight M_c of network chains (between adjacent junctions) derived from measurements of the equilibrium swelling ratio in cyclohexane and through the classical Flory-Rehner equation. Values of M_c are 2×10^4, 1.5×10^4, 2.2×10^4, and 6.1×10^4 g/mol for Samples A, B, C, and D, respectively. Comparison of these values of M_c with the precursor molecular weight of the labeled chains (600 000) ensured that anthracene was in the backbone of active chains in the networks after the crosslinking process. The four networks were characterized by stress-strain experiments [44]. Data points for Sample C (upper set of points) and Sample D (lower set of points) are presented in Fig. 4. The curves through the experimental points were calculated according to the Flory-Erman model of constrained junctions presented in Section IV-B. Values of the three parameters $\xi kT/V$, κ, and ζ that give the best fit to experimental data are reported in Table 1 for the four networks.

The reduced orientation function, $[S_x]$, calculated according to Eq. (32) from experimental measurements, is shown in Fig. 5 for Samples C and D. The experimental data were fitted with curves calculated according to the Erman-Monnerie model of segmental orientation [15] (combination of Eqs.

TABLE 1. Parameters Used in Theoretical Calculations of Stress and Orientation for Networks with Center-Labeled Chains

Sample	$\xi kT/V$, N/mm^2	κ	ζ	$D \times 10^2$ [a]	e
A	0.125	7	0.025	1.30	1.4
B	0.177	7	0.025	1.60	1.4
C	0.121	7	0.025	1.16	1.4
D	0.063	10	0.025	0.76	1.6

[a] At 298 K.

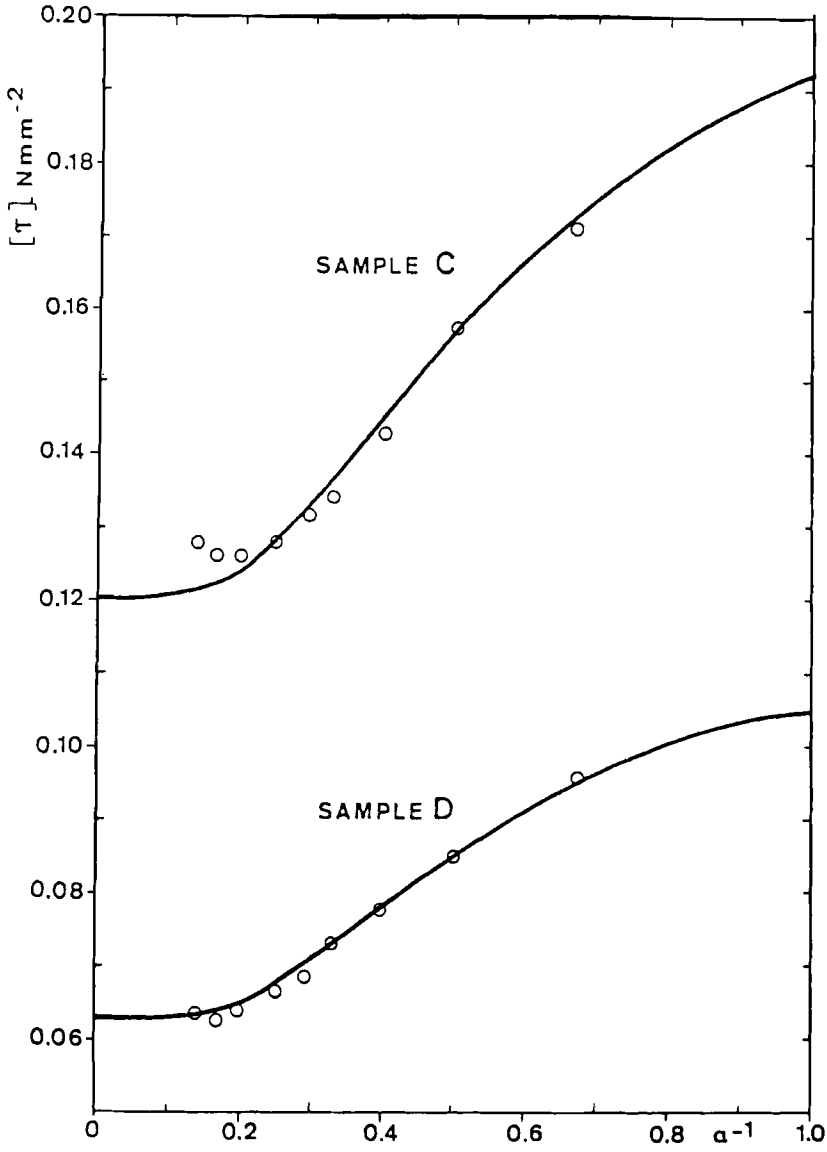

FIG. 4. Reduced stress, $[\tau]$, as a function of reciprocal extension ratio α^{-1} (Mooney-Rivlin plot) [44]. Points represent results of experiments for Sample C (upper set) and for Sample D (lower set). Solid curves were obtained by fitting experimental points to the Flory-Erman theoretical expression for reduced stress [2]. (Combination of Eqs. 13 and 16.) The parameters used in the fitting are given in Table 1.

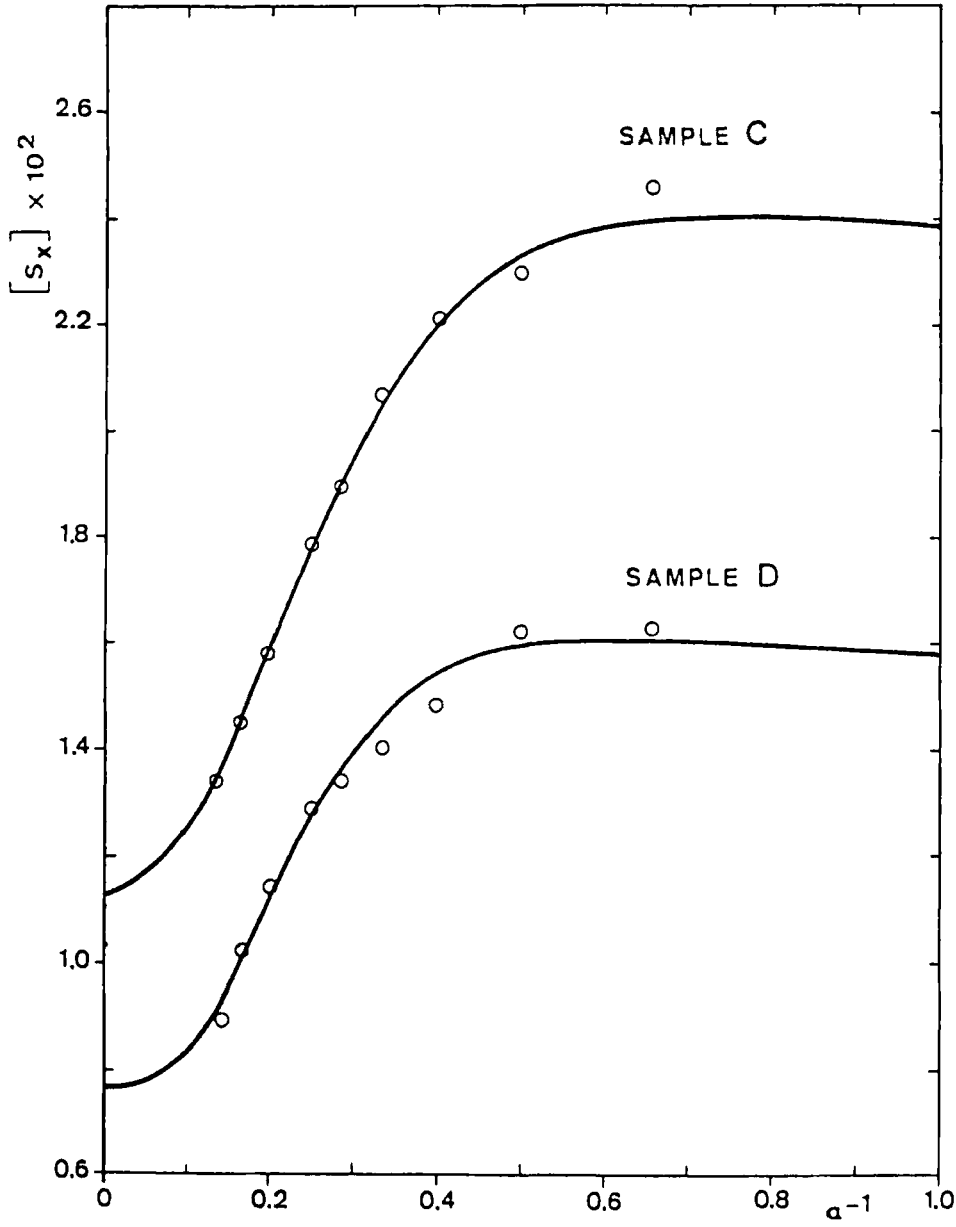

FIG. 5. The reduced orientation function, S_x, as a function of α^{-1} [44]. Points represent results of experiments for Sample C (upper set) and for Sample D (lower set). Solid curves were calculated according to the Erman-Monnerie model of segmental orientation [15]. The parameters used in the fitting are reported in Table 1.

30 and 32). Good agreement is reached between theory and experiment. According to the two curves obtained by the theory, the reduced orientation function remains approximately constant in the range $1 < \alpha < 2$. Above $\alpha = 2$, the curves converge steeply to the respective phantom values represented by the intercepts at $\alpha^{-1} = 0$. As with the Flory-Erman model for the stress-strain relationship, which suppresses the discrepancies observed between theoretical predictions and experiments for phantom or affine models, the Erman-Monnerie theory is successful in accounting for the decrease of the reduced orientation function when strain is increased.

The parameters D and e used in the fitting are reported in Table 1 for the four networks. More demanding is the comparison of data and theory in terms of the ratio of reduced orientation to reduced stress, $[S_x]$ to $[\tau]$, presented in Fig. 6 as a function of α for Samples C and D. The maxima observed in the set of experimental points coincide with the respective maxima in the curves obtained from theory. According to the theory, the limiting value of the intercept of $[S_x]/[\tau]$ at $\alpha^{-1} = 0$ in the absence of local intermolecular correlations should be the same for the two networks since both $[S_x]$ and $[\tau]$ scale with N^{-1} under the stated conditions (where N is the number of segments per chain between crosslinks). Experimental values of the intercept in Fig. 6 differ by about 20%. Inasmuch as intermolecular correlations do not contribute to stress [41], the observed difference in the ratio $[S_x]/[\tau]$ for Networks C and D indicates that the contribution of intermolecular correlations to segmental orientation is larger in less crosslinked systems.

The nonlinearity of the curves and data points in Fig. 6 clearly indicates that orientation is not proportional to stress and that stress cannot be accepted as a measure of segmental orientation in amorphous networks.

Finally, we have investigated the effect of temperature on segmental orientation and the Erman-Monnerie theoretical parameters. The variation of the orientation function with temperature for different extension ratios is shown in Fig. 7 for Sample B. $[S_x]$ decreases when the temperature increases. The data were fitted with theoretical expressions (Eq. 32) [15]. The values of κ and ζ, obtained from elasticity measurements, were 7 and 0.025, respectively (see Table 1). The value of e was chosen as 1.4, i.e., equal to that obtained for Sample A with identical chains. Thus the only fitting parameter remaining was D. At each temperature of measurement, its value was chosen to fit the whole set of data obtained at various values of α ranging from 1.5 to 3.5. Within the limit of accuracy of the fitting, the effect of temperature on D resulted in the linear dependence shown in Fig. 8. These observed changes in D may be attributed to the variation of D_{int} with temperature (see Eq. 23).

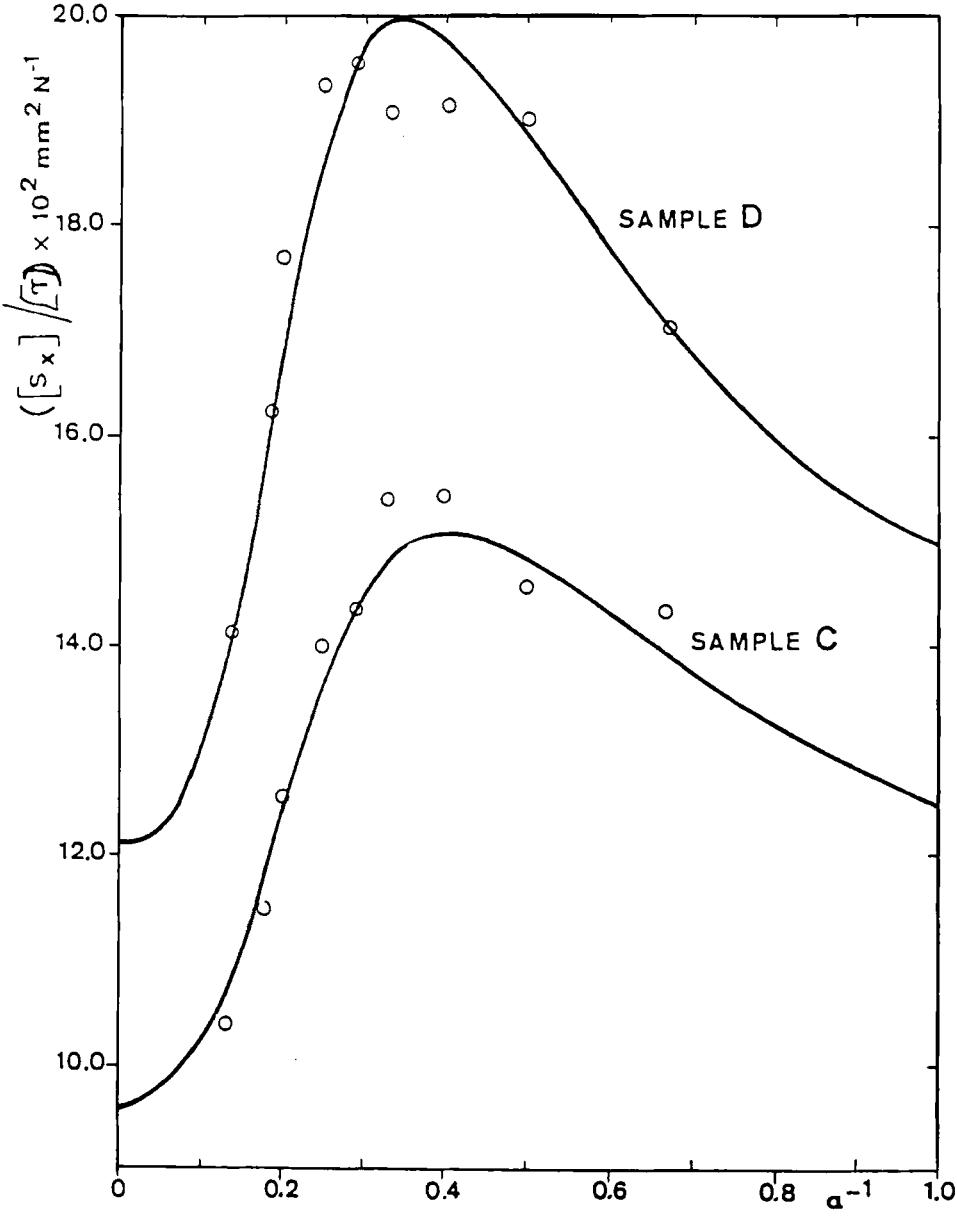

FIG. 6. Plot of the ratio of the reduced orientation to the reduced true stress as function of α^{-1} [44]. Points were obtained experimentally for Sample C (lower set) and Sample D (upper set). Solid curves were calculated with the parameters reported in Table 1 through a combination of Eqs. (13), (16), (30), and (32).

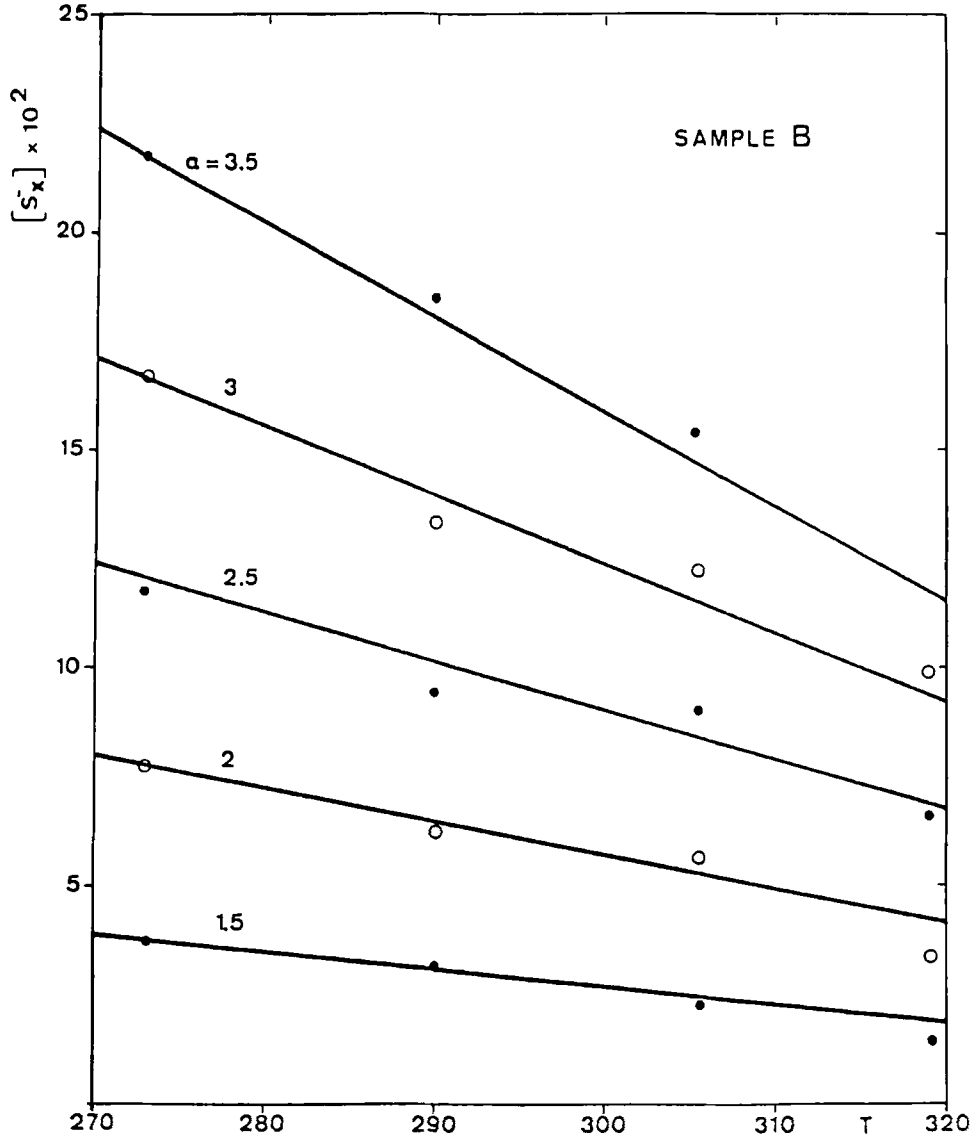

FIG. 7. Effect of temperature on reduced orientation at different extension ratios. Filled and open circles represent experimental data for Sample B [44]. Straight lines were obtained from theory as described in the text.

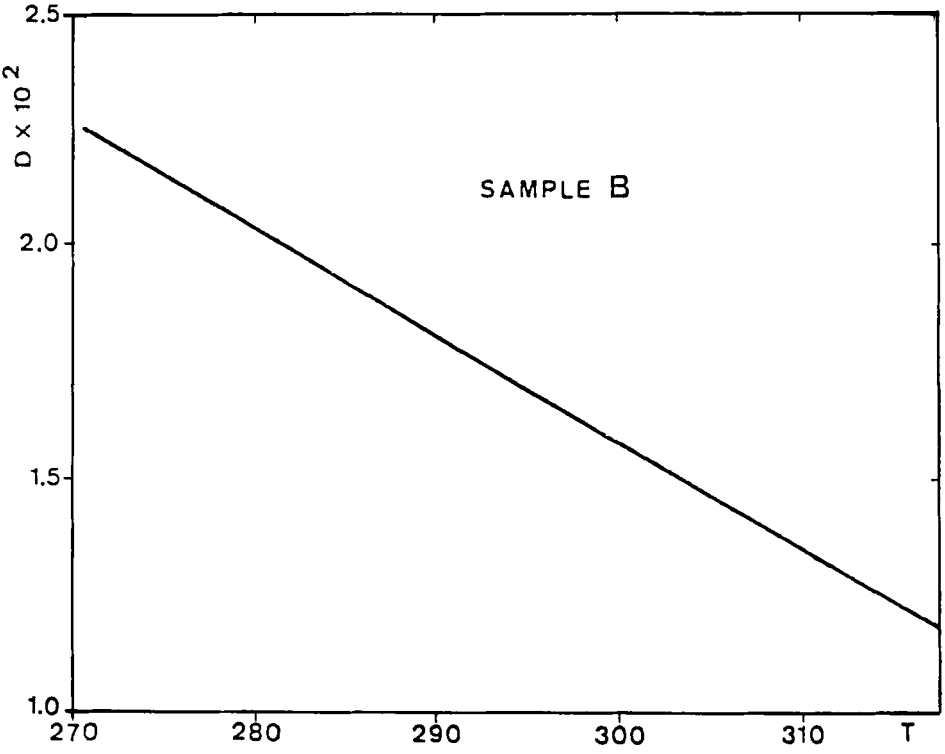

FIG. 8. Effect of temperature on the configurational factor, D, obtained from the fitting of data shown in Fig. 7 [44].

The later theory of segmental orientation presented in Section IV-C [15] was thus successfully tested. The decrease of reduced orientation function when strain increases can be accounted for by using the relationship between macroscopic and molecular network deformations derived from the Flory-Erman constrained junction model. The effect of temperature can be accounted for by changing parameter D of the orientation theory over a wide range (of the order of 2), which reflects the high sensitivity of local intermolecular correlations to temperature. Possible perturbation of intermolecular correlations due to the difference of the fluorescent label from segments of the main chain are included in the parameter e.

B. Orientation of End-Labeled Chains

After rapidly stretching a network, stress relaxation occurs mainly by disentanglements of dangling chains.

We have investigated the local segmental orientation of end-labeled chains in uniaxially stretched *cis*-polyisoprene networks at stress and orientation equilibrium [40, 45]. Anthracene orientation of center-labeled chains contained in bimodal network C ($\bar{M}_c = 2.2 \times 10^4$ g/mol) was compared to anthracene orientation of end-labeled chains contained in a similar bimodal network E ($M_c = 2.1 \times 10^4$ g/mol). The end-labeling was presented in Section III-C-1. The comparison may conveniently be made by defining a coupling function, f_d, as

$$f_d = S_{xd}/S_x, \tag{34}$$

where S_{xd} and S_x are the orientation functions for the dangling and network chains, respectively. The value of f_d may vary between 0 and 1, where the latter denotes complete orientational coupling of the dangling chains to the network chains, and the former indicates that there is no orientational coupling between the two. The coupling function corrected for the difference in M_c of the networks [45] is presented in terms of the extension ratio in Fig. 9. These data indicate that the coupling function is very strong, being ~0.96-0.97 for values of α between 1 and 5. The curve through the experimental points indicates that the degree of coupling is independent of extension up to $\alpha = 5$ and shows a progressive decrease at higher extensions, probably due to the finite extensibility of network chains that occurs at such high values of α.

In recent experiments on deuterated poly(dimethylsiloxane) (PDMS) chains dissolved in an unlabeled PDMS network [47, 48]. ^{2}H-NMR study of the free chains in the deformed network [47] indicated strong segmental orientation (similar results were obtained with polybutadiene [49]), whereas neutron-scattering experiments [48] showed no evident anisotropy of the free chains. This follows from the fact that a sufficiently flexible chain may be subdivided into sequences of bonds in which each sequence is uncorrelated with the neighboring sequences. Therefore, local sequence orientation can be observed without any overall chain anisotropy.

C. Orientation of Flexible and Rigid Probes

Analysis of data on orientational correlations obtained by various techniques shows that intermolecular orientational correlations between chain

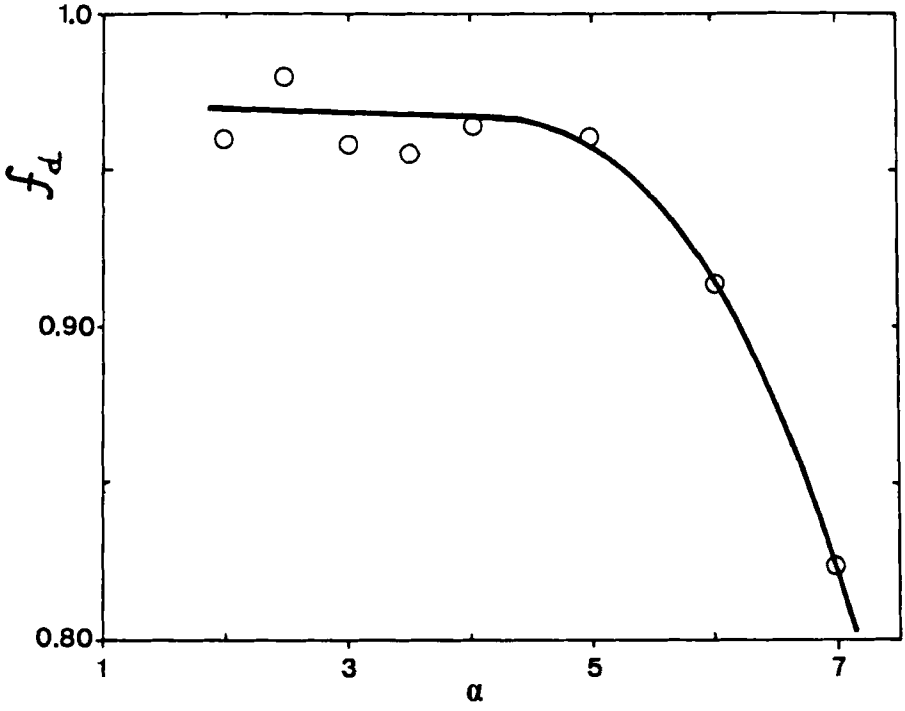

FIG. 9. Coupling function f_d for dangling chain ends (defined by Eq. 34) presented in terms of the extension ratio [45].

segments are significant in amorphous polymeric systems in the bulk state and that they diminish strongly upon dilution with isotropic solvents and that orientational correlations of solvent molecules with segments of the polymer chains depend predominantly on the shape anisotropy of the solvent molecules [33, 50-53]. The extent of correlation among the solvent molecules and the chains has been observed to be significant, even with solvent molecules of low anisotropy and at high degrees of dilution.

The specific aim of the study presented in this Section was to analyze orientational correlations between unattached flexible probes of different lengths (C_n probes shown in Fig. 3b) and network chains at various degrees of uniaxial extension of the network [46].

We have compared the anthracene orientation of the center-labeled chains of Sample B (see Section V-A) with the anthracene orientation of flexible

probes C_n inserted in polyisoprene networks of similar structure. The strength of orientational correlation may again be described by the coupling function f_p, now defined as

$$f_p = S_{xu}/S_x, \tag{35}$$

where S_{xu} and S_x are the orientation functions of the unattached flexible probes and the network chains, respectively.

It was shown [46] that f_p was independent of extension ratio for $\alpha \geqslant 3$. Values of f_p at high α are presented in Fig. 10 as a function of the parameter n, which is approximately proportional to the number of successive carbon bonds in the probes. Points denote the experimental data. The solid line is obtained by least-squares fit to the data points. It is clearly seen in Fig. 10 that the degree of coupling is proportional to the length of the probes and varies between 0.4 and 0.7.

On the other hand, orientation measurements on rigid rod probes (shown in Fig. 3c) dissolved in similar networks showed that the coupling function f_p varies inversely with probe length and depends strongly on α, as illustrated in Fig. 11 [54]. Estimates based on statistical analysis of polyethylene chains [23] show that the average length of the C_M probes along the major direction vary between 0.8 and 1.7 nm for $n = 2$ to 16. The lengths of the rigid polyene probes, on the other hand, were 1.15, 1.40, and 1.65 nm. This comparison indicates that the main difference between the observed behavior of the C_n and polyene probes lies in the flexibility of the former and the stiffness of the latter. Such stiffness could lead to selective correlation of the rod probes with specific configurational sequences of the *cis*-1,4-polyisoprene chains of the network [54, 55].

VI. CONCLUSIONS

The studies reported here on the segmental orientation of uniaxially stretched rubbery networks show that stationary fluorescence polarization is a very powerful technique for investigation of the molecular behavior of polymers.

As only the orientation behavior of the labeled species is observed, specific topological entities of the network structure, like centers of active chains or ends of dangling chains, can be looked at. The possibility of insertion of flexible or rigid probes of different lengths may be used to characterize orientational coupling between these probes and the polymer matrix. In the field of rubberlike elasticity, characterization of segmental orientation may serve to validate and improve elasticity models derived from mechanical properties. Specifically,

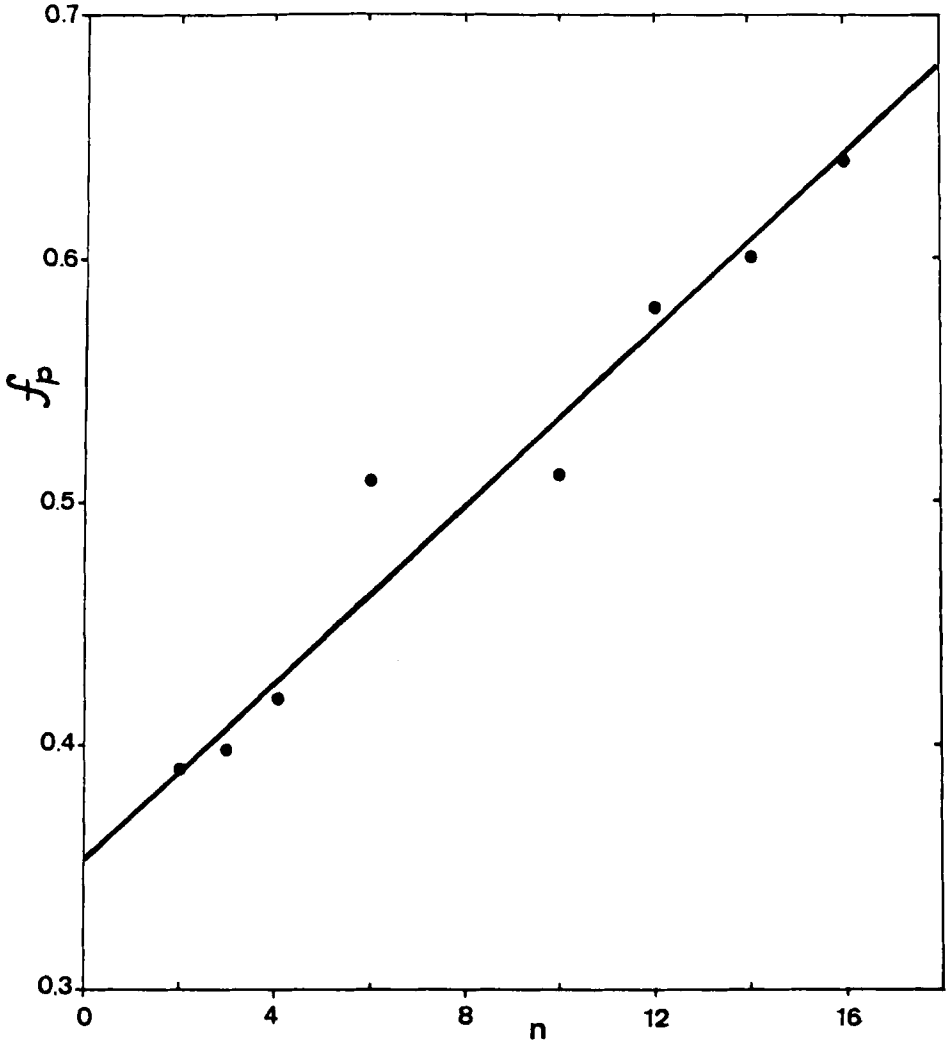

FIG. 10. Coupling function f_p for flexible probes in polyisoprene networks presented as a function of probe length n [46]. The straight line is the least-squares line through the experimental points.

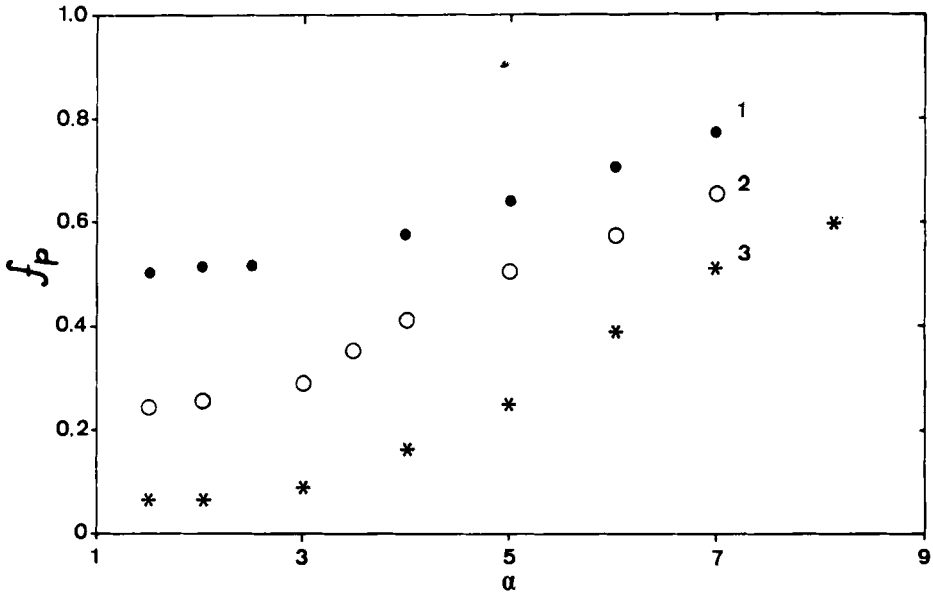

FIG. 11. Coupling function f_p for rigid probes in polyisoprene networks. Points represented by the Sets 1, 2, and 3 are experimental data for DPBD (●), DPHT (○), and DPOT (*), respectively [54].

we have successfully tested the Erman-Monnerie theory of segmental orientation based on a strain function including the nonaffine molecular deformation consecutive to restrictions on junction fluctuations and distortions of constraint domains and a configurational factor accounting for local intermolecular orientational correlations.

ACKNOWLEDGMENT

Collaboration with Jean-Pierre Jarry (Rhône-Poulenc, Miribel) is greatly appreciated.

REFERENCES

[1] G. Ronca and G. Allegra, *J. Chem. Phys., 63,* 4990 (1975).
[2] P. J. Flory and B. Erman, *Macromolecules, 15,* 800 (1982).
[3] R. S. Stein, F. H. Holmes, and R. V. Tobolsky, *J. Polym. Sci., 14,* 443 (1954).
[4] A. N. Gent, *Macromolecules, 2,* 262 (1969).
[5] T. Ishikawa and K. Nagai, *J. Polym. Sci., Part A-2, 7,* 1123 (1969).
[6] L. Monnerie, *Faraday Symp. Chem. Soc., 18,* 57 (1983).
[7] I. M. Ward, *Structure and Properties of Oriented Polymers,* Applied Science Publishers, London, 1975.
[8] J. P. Jarry and L. Monnerie, *Macromolecules, 12,* 927 (1979).
[9] J. P. Jarry and L. Monnerie, *J. Polym. Sci., Polym. Phys. Ed., 16,* 443 (1978).
[10] L. Monnerie and J. P. Jarry, *Ann. N. Y. Acad. Sci., 366,* 328 (1981).
[11] J. P. Jarry, P. Sergot, C. Pambrun, and L. Monnerie, *J. Phys. E: Sci. Instrum., 11,* 702 (1978).
[12] M. G. Krakoviak, E. V. Anufrieva, and Yu. Ya. Gotlieb, *Adv. Polym. Sci., 40,* 1 (1981).
[13] B. Valeur and L. Monnerie, *J. Polym. Sci., Polym. Phys. Ed., 14,* 11 (1976).
[14] C. K. Yeung, Thesis, Université Paris VI, 1983.
[15] B. Erman and L. Monnerie, *Macromolecules, 18,* 1985 (1985).
[16] J. E. Mark, *Adv. Polym. Sci., 44,* 1 (1982).
[17] J. P. Queslel and J. E. Mark, *J. Polym. Sci., Polym. Phys. Ed., 22,* 1201 (1984).
[18] A. Charlesby and S. H. Pinner, *Proc. R. Soc. London, A249,* 367 (1959).
[19] D. S. Pearson and W. W. Graessley, *Macromolecules, 11,* 528 (1978).
[20] M. Hoffman, *Makromol. Chem., 183,* 2191 (1982).
[21] P. J. Flory, *Proc. R. Soc. London, A351,* 351 (1981).
[22] P. J. Flory, *Br. Polym. J., 17,* 1 (1985).
[23] D. Y. Yoon and P. J. Flory, *J. Chem. Phys., 61,* 5366 (1974).
[24] P. J. Flory and V. W. C. Chang, *Macromolecules, 9,* 33 (1976).
[25] B. E. Eichinger, *Annu. Rev. Phys. Chem., 34,* 359 (1983).
[26] F. T. Wall, *J. Chem. Phys., 11,* 527 (1943).
[27] H. M. James and E. Guth, *Ibid., 15,* 669 (1947).
[28] M. Mooney, *J. Appl. Phys., 11,* 582 (1940).
[29] G. Allen, M. J. Kirkham, J. Padget, and C. Price, *Trans. Faraday Soc., 67,* 1278 (1971).
[30] G. Gee, *Ibid., 50,* 881 (1954).

[31] P. J. Flory, *Polymer, 20,* 1317 (1979).
[32] B. Erman and P. J. Flory, *Macromolecules, 15,* 806 (1982).
[33] B. Erman and P. J. Flory, *Ibid., 16,* 1607 (1983).
[34] J. P. Queslel, P. Thirion, and L. Monnerie, *Polymer, 27,* 1869 (1986).
[35] B. Erman, *J. Polym. Sci., Polym. Phys. Ed., 19,* 829 (1981).
[36] L. R. G. Treloar, *Br. Polym. J., 14,* 121 (1982).
[37] L. R. G. Treloar, *The Physics of Rubber Elasticity,* Clarendon, London, 1975.
[38] W. Kuhn and F. Grun, *Kolloid-Z., 101,* 248 (1942).
[39] M. H. Liberman, Y. Abe, and P. J. Flory, *Macromolecules, 5,* 550 (1972).
[40] J. P. Queslel, Thesis, Université Paris VI, 1982.
[41] J. P. Jarry.and L. Monnerie, *J. Polym. Sci., Polym. Phys. Ed., 18,* 1879 (1980).
[42] P. J. Flory, *Rubber Chem. Technol., A8,* 513 (1975).
[43] K. Nagai, *J. Chem. Phys., 40,* 2818 (1964).
[44] J. P. Queslel, B. Erman, and L. Monnerie, *Macromolecules, 18,* 1991 (1985).
[45] B. Erman, J. P. Queslel, and L. Monnerie, *Polymer,* Submitted.
[46] J. P. Queslel, B. Erman, and L. Monnerie, *Ibid.,* Submitted.
[47] B. Deloche, A. Dubault, J. Herz, and A. Lapp, *Europhys. Lett., 1,* 629 (1986).
[48] F. Boue, B. Farnoux, F. Bastide, A. Lapp, J. Herz, and C. Picot, *Ibid., 1,* 637 (1986).
[49] M. M. Jacobi, R. Stadler, and W. Gronski, *Macromolecules, 19,* 2884 (1986).
[50] E. W. Fischer, G. R. Strobl, M. Dettenmaier, M. Stamm, and N. Steidl, *Faraday Discuss. Chem. Soc., 68,* 26 (1979).
[51] M. Fukuda, G. L. Wilkes, and R. S. Stein, *J. Polym. Sci., Polym. Phys. Ed., 9,* 1417 (1971).
[52] G. Gelhard, G. Rehage, and J. Schwarz, *Br. Polym. J., 9,* 156 (1977).
[53] R. T. Ingwall, E. A. Czurylo, and P. J. Flory, *Biopolymers, 12,* 1137 (1973).
[54] B. Erman, J. P. Jarry, and L. Monnerie, *Polymer, 28,* 727 (1987).
[55] J. H. Nobbs, D. I. Bower, and I. M. Ward, *J. Polym. Sci., Polym. Phys. Ed., 17,* 259 (1979).